

Calculations of Earth Surface Deformation Due to Oil Extraction in Southern Iraq Using DInSAR

Ali A. Hussein^{1*}, Auday H. Shaban¹ and Najah A. Abd²

¹Department of remote sensing and GIS, College of Science, University of Baghdad, Baghdad, Iraq

²Department of Geology, College of Science, University of Baghdad, Baghdad, Iraq

*Corresponding author: Ali.Ayad2209m@sc.uobaghdad.edu.iq

Abstract

Oil extraction is a crucial industry for Iraq, significantly contributing to the country's economy, particularly in Basra Governorate. However, intensive extraction activities can lead to ground deformation, manifesting as subsidence and uplifts, which may impact infrastructure and the environment. This study investigates ground deformations caused by oil extraction in the Rumaila oilfield, one of Iraq's major oil-producing areas, located in southern Iraq. The study employed Differential Interferometric Synthetic Aperture Radar (DInSAR) techniques using Sentinel-1 SAR data from the European Space Agency. To analyze these deformations, DInSAR allows for precise measurement of surface deformation by calculating displacement differences between pairs of SAR images over time, making it an effective tool for monitoring subtle ground movements. The Rumaila oilfield, which consists of northern and southern sections, was chosen due to its high oil production and its significance to Iraq's economy. The results revealed significant deformation in the Rumaila oilfield, with a subsidence rate that ranged between -1.53 and -1.64 m over six years. The southern Rumaila oilfield displayed more substantial deformation (-1.64 m), which represents the maximum, correlating with higher extraction rates, while the northern field exhibited relatively minor deformation due to lower extraction levels. This distinction highlights the impact of extraction intensity on ground stability within the field.

Article Info.

Keywords:

Deformation, Rumaila, Remote Sensing, InSAR, Oilfield.

Article history:

Received: Nov. 24, 2024

Revised: Feb. 03, 2025

Accepted: Feb. 24, 2025

Published: Mar. 01, 2026

1. Introduction

Oil is one of the most important hydrocarbon materials in daily human life[1]. It is extracted from the Earth's crust by drilling wells. Oil is refined to produce a variety of products; oil and its derivatives are used as fuel for vehicles, for cooking, and for generating thermal and electrical energy[2, 3]. Iraq is one of the oil-producing countries; a significant part of its economy is based on the extraction and exportation of oil, [4, 5]. Consequently, over time, oil extraction at high production rates leads to ground deformations. Ground deformations are the uplift or subsidence of the Earth's crust; these deformations also result from natural factors, such as earthquakes and volcanic activity, as well as human activities like groundwater extraction and landfilling. Oil extraction is one of these human activities that alter the nature of the Earth's surface in addition to causing environmental pollution [6-10]. Satellite data can be obtained for different time periods, which facilitates the monitoring and calculation of deformations [11, 12]. One of the most important data types used in studying deformations is radar imaging, where synthetic aperture radar(SAR) images represent a very important information source in this study, as they can calculate the height differences between two images (before and after), and this difference represents the deformation [13-15].

Many researchers have conducted similar studies in various locations worldwide, and the following is a review of the most important of these studies.

In 2010, Chang et al. examined surface deformation in northern Taiwan for 15 years, including the Taipei Basin and surrounding mountains, using ERS-1, ERS-2, and ENVISAT SAR images. Although Dinsar effectively monitor dense basin and vegetation,

its application is limited in mountainous areas, leading to the use of PSInSAR, helping to successfully reduce noise and provide more accurate deformation data. The analysis revealed a slight uplift in the Western Foothills, Tatun Volcanoes, Linkou Tableland, and Taoyuan area, subsidence at the border of the Taipei Basin, and a slight uplift rebound in the center of the basin. The displacements along the Shanchiao, Chinshan, and Kanchiao Faults were noticeable, while the movements along the Taipei, Hsinchuang, and Nankang Faults were minimal. The comparison between DInSAR, PSInSAR, and levelling data showed a strong correlation, confirming the reliability of radar interferometry for surface deformation monitoring [16].

In 2011, Shirzae et al. studied the dormant Damavand volcano in northern Iran. The study was an analysis of long-term volcanic deformations. The study utilized Interferometric Synthetic Aperture Radar (InSAR) to generate a deformation time series from 2003 to 2008. The results showed lateral extension of the volcano at a rate of up to ~ 6 mm/year, accompanied by subsidence at the summit at a rate of up to ~ 5 mm/year, with the eastern flank exhibiting more significant movement than the western flank. This phenomenon is interpreted as slow, long-term gravity-driven deformation, indicating that the Magma activity is not necessary for attractive spread. This finding highlighted the importance of identifying such deformations for volcanic hazard assessment, even in dormant volcanoes [17].

In 2013, Wöppelmann et al. examined land subsidence along Alexandria's coastline, Egypt, using GPS and InSAR data from 49 Envisat SAR scenes (2003–2010). Results showed moderate subsidence averaging 0.4 mm/year, with localized rates up to 2 mm/year, lower than previous estimates (>3 mm/year). Mariut Lake's shallow waters subside at ~ 1 cm/year, while the city center remains stable or subsides slightly (~ 1 mm/year), especially around the former sandy tombolo of Pharos. On long timescales (centuries to millennia), subsidences were driven by tectonics, earthquakes, and fault collapse, while on shorter timescales (decades to centuries), steady subsidence results from natural sediment compaction. GPS data from CEAlex (2001–2008) confirmed minimal vertical movement (0.05 ± 0.29 mm/year), validating the PSI analysis. The study highlighted the value of combining InSAR and GPS for precise subsidence monitoring, providing crucial insights for coastal stability and hazard assessment [18].

In 2017, Milillo et al. focused on the Mosul Dam, the largest hydraulic structure in Iraq located on the Tigris River, and examined its ongoing destabilization and deformation monitoring. Utilizing Synthetic Aperture Radar (SAR) data from COSMO-SkyMed and Sentinel-1A, along with historical Envisat ASAR data from 2004 to 2010. The study provided a comprehensive multi-sensor analysis of the dam's structural changes over time. The results revealed a significant subsidence with minimal horizontal motion. Between 2004 and 2010, Envisat data recorded a Line-Of-Sight (LOS) deformation rate of -10 mm/year ± 6 mm/year, translating to a vertical subsidence of -10.8 mm/year. A regression analysis covering from 2012 to 2015 indicated a maximum deformation rate of -7.8 ± 1.8 mm/year LOS (-9.6 mm/year vertical), while between December 2012 and December 2013, subsidence rates remained below 2.3 ± 1.8 mm/year. The study also found that the deformation slowed between 2012 and 2014 but resumed in August 2014 when grouting operations ceased due to the temporary takeover of the dam. This research highlighted the critical role of multi-sensor SAR data in capturing high-resolution spatial and temporal details of structural deformations. By integrating historical and contemporary satellite datasets, the study underscored the importance of continuous monitoring for assessing the long-term stability of infrastructure and mitigating potential risks [19].

In 2022, Shi et al. focused on the Lost Hills oilfield in California, detailing its geological context and oil exploration history from 1995 to 2011, depending on a new

approach using multi-track SAR data to calculate vertical deformation, overcoming the limitations of traditional methods. The experimental results showed a maximum vertical deformation rate of 20 mm/year in the uplift region and 90 mm/year [20].

In 2023, Xu et al. discussed the deformation due to hydrocarbon extraction and other geological effects. In Karamay Oilfield, China, the interferometric synthetic aperture radar data was used between 2018 and 2020. Their results showed average deformation rates ranging from -20 to 30 mm/year. The maximum uplift rate recorded was 58.3 mm/year, while the maximum subsidence rate was -36.6 mm/year [21].

The purpose of this study is to calculate and understand the amounts of deformation occurring in areas of high oil extraction and to monitor and estimate them using remote sensing data, as this data and these techniques play a very effective and significant role in this type of study.

1.1. Study Area

The Rumaila oilfield is located in the southern part of Basra Governorate, with the majority of it situated in the Al-Zubair district and parts of the Al-Qurna district, with the following coordinates: longitudes ($47^{\circ}5'15''\text{E}$ and $47^{\circ}40'55''\text{E}$) and two latitudes ($30^{\circ}47'15''\text{N}$ and $30^{\circ}5'4''\text{N}$) as illustrated in Fig. 1.

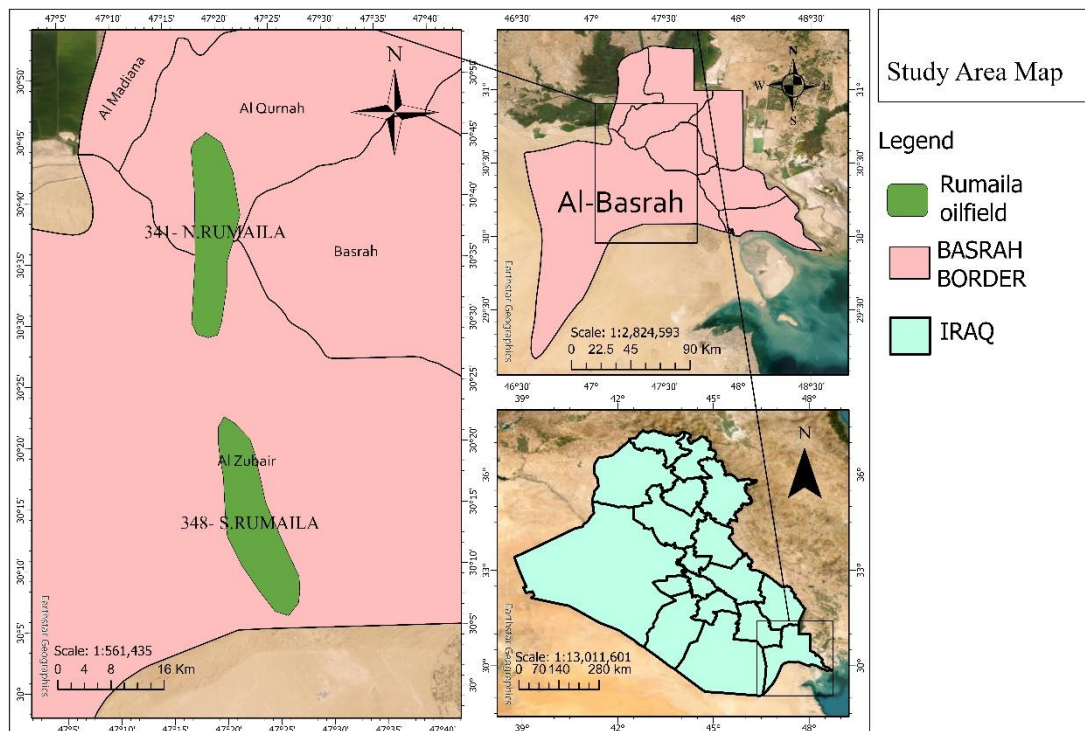


Figure 1: Study area map.

Fig. 1 shows the study area map representing the Rumaila oilfield, which is illustrated by the green area. Oil is available in many provinces of Iraq, but Basra Governorate is considered the primary source, accounting for 59 % [22, 23]. Basra is one of the most important oil regions in Iraq, as it contains oil wealth and is among the most prominent oil regions in the world [2]. Oil in Basra plays a vital role in the Iraqi economy, as it is considered a primary source of income and development [24, 25].

Basra Governorate is characterized by a large number of geological formations that contain oil and natural gas. Among these fields is the Rumaila oilfield, which is divided

into parts: the northern and the southern [26, 27]. This field represents the largest proportion of Basra's oil, accounting for approximately 80-85 % [28].

2. Materials and Methods

Statistical, spatial, and remote sensing data were used in this work. Deformations were determined using the DInSAR method, as illustrated in Fig. 2.

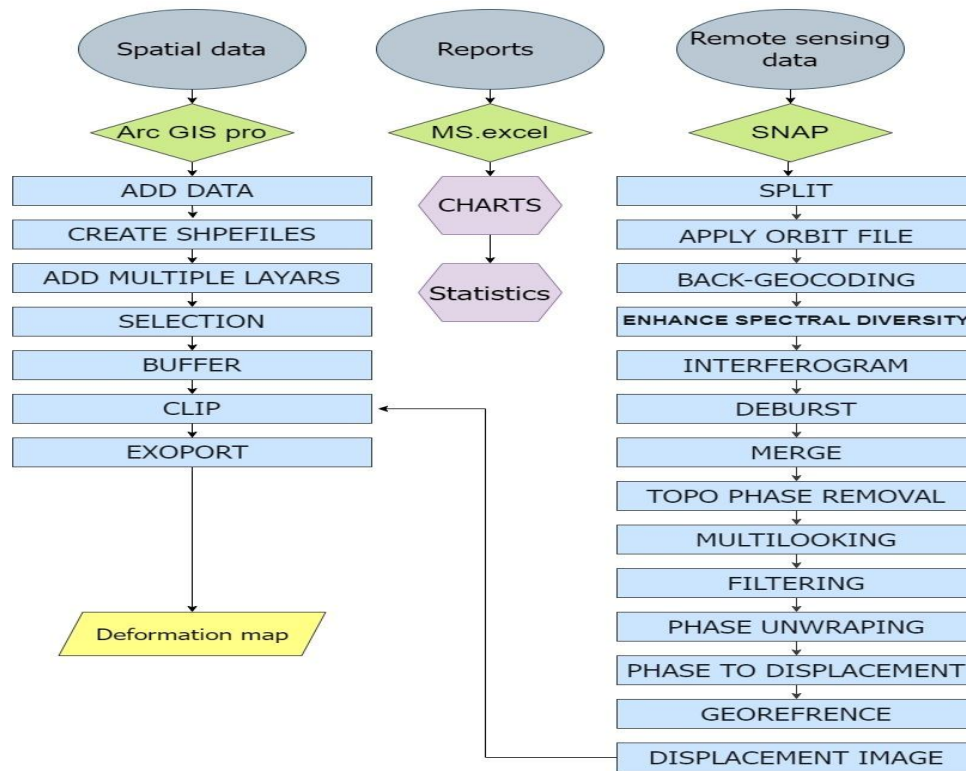


Figure 2: Methodology flow chart.

2.1. Dataset

Various types of data were used in this study. The first group of data consisted of spatial data, which included maps of oil fields and administrative boundary data for the Basrah Governorate, encompassing districts, sub-districts from diva_GIS website [29], and locations of oil wells. The second data group was statistical data on oil extraction quantities in Iraq, obtained from OPEC reports. The third type of data involved remote sensing, specifically SAR SLC IW band C radar images for the period between June 2017 and September 2023 which were used to calculate deformations. This data is available on the official website of the European Space Agency (ESA). The sentinel 1 SAR data are: S1A_IW_SLC__1SDV_20170611T024644_20170611T024711_016980_01C451_A5DE S1A_IW_SLC__1SDV_20230920T024726_20230920T024753_050405_0611C9_720F. Details are shown in Table 1. The sentinel raw data is shown in Fig. 3.

Table 1: SAR data characteristics.

Image	Polarization	Direction	Sub type	Band	Type and acquisition
September 2023	VV+VH	Descending	S1A	C	SLC_IW
June 2017	VV+VH	Descending	S1A	C	SLC_IW



Figure 3: SAR raw data.

2.2. Methodology

After obtaining the data mentioned in the previous paragraph, a set of programs was used, including SNAP version 9, ArcGIS Pro version 3, and Excel for creating graphs, as follows:

SNAP was used to analyze SAR radar images from the Sentinel-1 satellite to generate interferograms to calculate deformations by determining the phase difference between two images [30]. This phase difference is then converted into displacement, representing the deformation, typically manifested as subsidences or uplifts. The images were processed through several steps including orbital, spatial, and spectral corrections to achieve the most accurate results possible. After the correction processes, the two images emerged to calculate the phase difference, which is the most critical step in obtaining results. This process utilized Digital Elevation Models (DEMs) generated from Shuttle Radar Topography Mission (SRTM), which are automatically downloaded during the processing [31]. Once the phase difference between the two images was obtained, the deformation was calculated through the phase-to-displacement step, followed by geo-referencing the resulting image and exporting it to extract the required area and complete the process in ArcGIS Pro.

In ArcGIS Pro, maps were displayed, and oil fields were drawn based on the map, as shown in Fig. 4, identifying the fields to be studied, namely the North and South Rumaila oilfields. A buffer zone of 10 km was created around each field to examine the extent of the deformations around the field, as shown in Fig. 5. The resulting image from the calculations in SNAP was classified into colour gradients from green to red to identify the most affected areas. Finally, the final maps representing the results were extracted.

Statistical data for Iraq were extracted from OPEC reports, which were processed in Excel, providing information on the production rate in (thousand barrels/ day) (tb/d) to determine the quantities of oil extracted and to compare the North and South Rumaila oilfields.

Fig. 5 shows Iraq's oil production from 2017 to 2023; this period witnessed a very high oil production in Iraq at a rate of 4340 tb/d. Based on OPEC reports, the third quarter of the year 2019 witnessed the highest percentage of oil production, reaching 4750 tb/d, while the lowest production rate was in the third quarter of 2020, reaching 3690 tb/d.

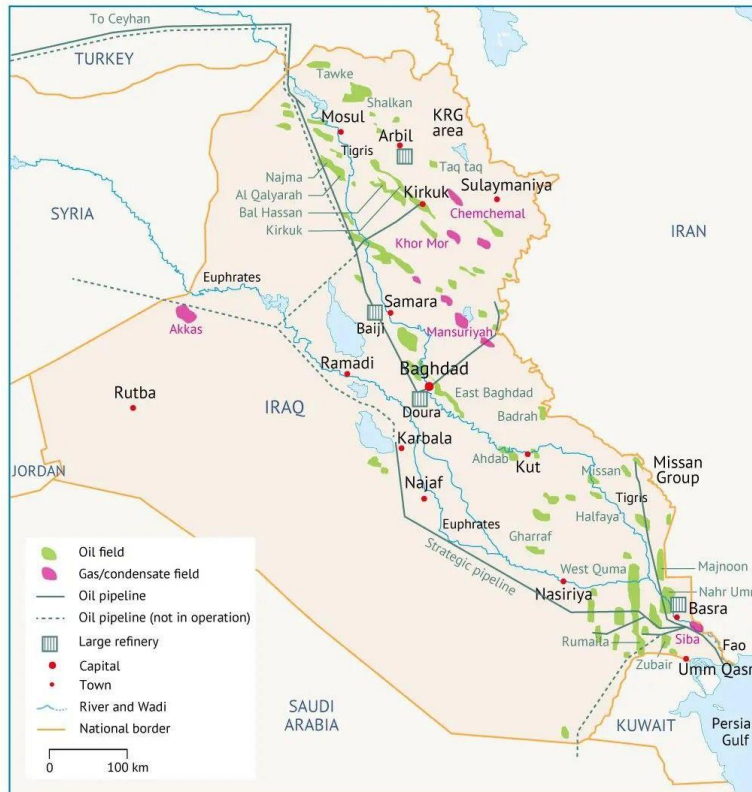


Figure 4: Map of Numerous oil Fields in Iraq [22].

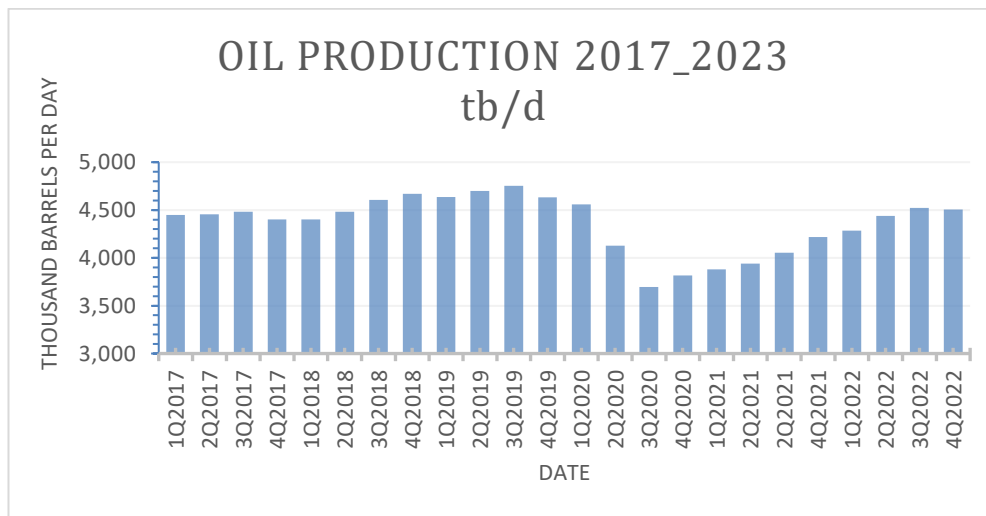


Figure 5: Oil production in Iraq 2017 to 2023[32].

3. Results and Discussion

In the deformation studies, the effect does not appear only at the exact location of the damage but also affects the surrounding areas. Therefore, a 10-kilometer radius around the oil fields was selected to study the impact of the deformations, as shown in Fig. 6. the phase difference map with values ranged from -3.13 to 3.13 phase unit. This phase must be unwrapped while this process done through snaphu in as shown in Fig. 7. The next step to calculate the real deformation, as shown in Fig. 8.

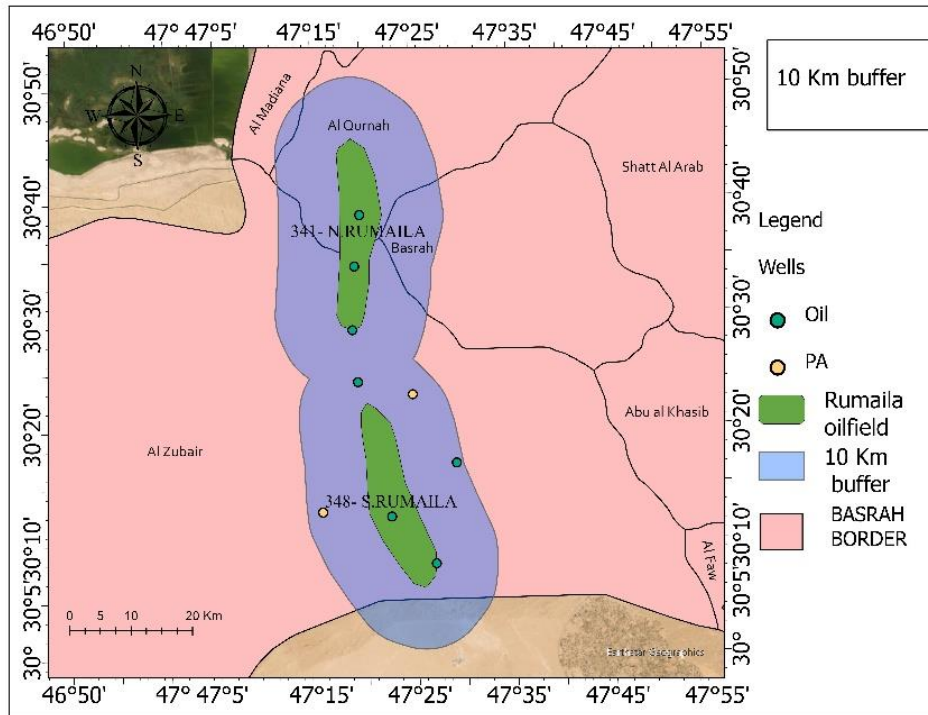


Figure 6: 10Km buffer zone.

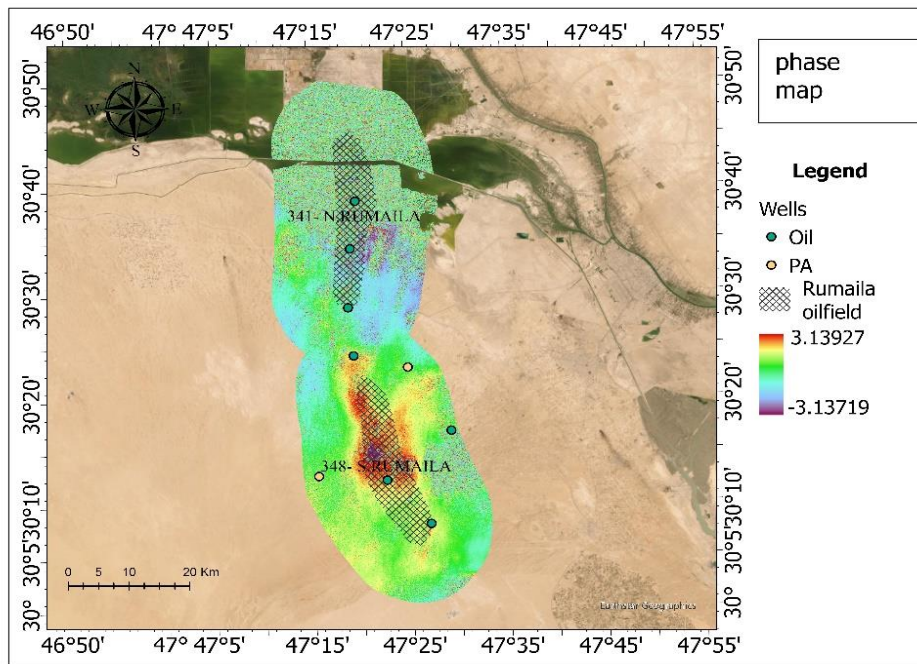


Figure 7: The phase map.

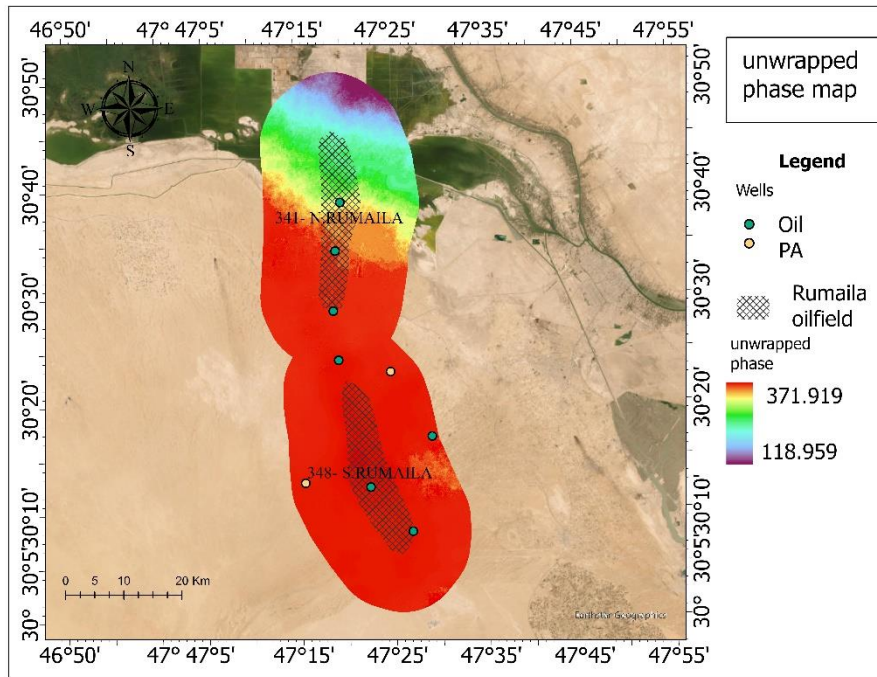


Figure 8: Unwrapped phase.

Fig. 8 illustrates the unwrapped phase; the red part indicates the highest deformation. To measure the deformation in metric unit the (phase to displacement) operation is used. The results showed that the area surrounding the northern and southern Rumaila oilfields witnessed a gradual subsidence, the highest of which reached -1.67 to 0 meters, as shown in Fig. 9.

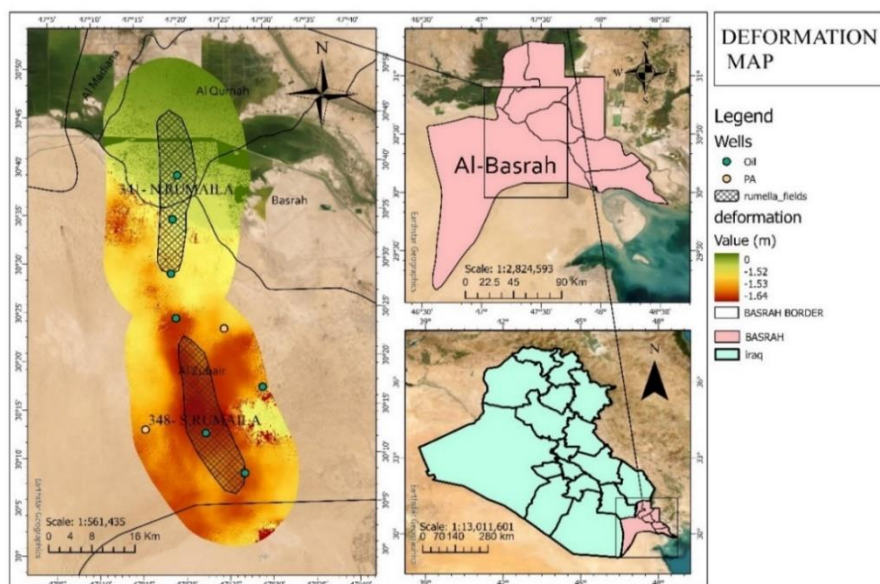


Figure 9: Deformation map.

Fig. 9 shows the deformation that the area was exposed to, where the deformations were represented by color ranging from dark red to dark green. The green colour represents the lowest percentage of deformation, while the red colour represents the highest degree of subsidence. The South Rumaila oilfield experienced the highest values of decline, represented by the red and orange colours, which ranged between -1.53 and -1.64 meters, due to the higher quantities of oil being withdrawn from it, as approximately 1.2 million barrels were withdrawn from the South Rumaila oilfield. In contrast, the North

Rumaila oilfield showed lower deformation rates, represented by the light yellow and green colours, as the quantities of oil drawn from this field were much less, amounting to approximately 200 thousand barrels per day. This led to less deformation, ranging from 0.3- to 1.45- meters for approximately six years. As for the dark green colour, it represents water bodies, as it is known that the water surface level did not change, and therefore the deformation value was zero. During the study period from 2017 to 2023, no significant seismic activity was recorded in Basra Governorate. According to previous studies, surface deformation has been observed even with much lower extraction volumes over significantly shorter periods. This strongly indicates that the observed deformation in the Rumaila oil field is indeed a result of extensive oil extraction during the study period. The deformation range represented by the green areas indicates minor changes or relative stability, while the red regions represent more significant deformations. In this study, the maximum deformation was 20 cm, with positive values indicating uplift and negative values indicating subsidence.

4. Conclusions

Significant deformation linked to extraction: Intensive oil extraction in the Rumaila oilfield, particularly in its southern section, has caused notable ground deformation, with subsidence reaching up to -1.67 meters over six years. DInSAR Effectiveness: Differential Interferometric Synthetic Aperture Radar (DInSAR) proved effective in monitoring and measuring these deformations accurately, highlighting its value for analyzing ground stability in oil extraction zones. If extraction at these high rates continues, it will significantly impact infrastructure. Therefore, it is crucial to reduce extraction as much as possible and shift towards clean energy sources. Recommendation for ongoing monitoring: Continued remote sensing and monitoring are recommended to assess long-term impacts on infrastructure and to support sustainable practices that minimize environmental and structural risks in the region. Impact of extraction intensity: The study found a clear correlation between extraction intensity and ground deformation, with higher extraction rates in the southern Rumaila oilfield leading to greater subsidence, illustrating the necessity of balanced extraction practices to mitigate surface impact. Currently, water is being injected instead of oil to maintain balance. However, the results show that deformations are ongoing, which points to the need for alternative solutions. Future research should focus on other oil fields in Iraq to compare extraction methods and determine their impact on surface deformations.

Conflict of Interest

Authors declare that they have no conflict of interest.

References

1. T. T. Al-Hameedi, D. U. K. Abbas, and L. E. George, *J. Pet. Explor. Prod. Technol.*, **9**, 1339 (2019). <https://doi.org/10.1007/s13202-018-0581-x>.
2. D. U. K. Abbas and L. E. George, *TELKOMNIKA*, **20**, 383 (2022). <https://doi.org/10.12928/telkonnika.v20i2.22462>.
3. D. Jumaah, *J. Eng. Res.*, (2021). <https://doi.org/10.36909/jer.11989>.
4. S. F. Behadili and B. H. Sayed, *Iraqi J. Sci.*, **60**, 2308 (2019). <https://doi.org/10.24996/ijs.2019.60.10.25>.
5. T. L. Jassim, *AgBioForum*, **23**(1), 1 (2021). <https://orcid.org/0000-0002-4928-3430>.
6. K. A. Al-Aasadi, A. A. Alwaeli, and H. A. Kazem, *J. Novel Appl. Sci.*, **4**, 82 (2015).
7. Z. A. Khaleel, A. H. Shaban, and A. A. Al Maliki, *J. Phys.: Conf. Ser.*, **2754**, 012025 (2024). <https://doi.org/10.1088/1742-6596/2754/1/012025>.
8. Z. A. Khaleel, A. H. Shaban, and A. A. Al Maliki, *J. Phys.: Conf. Ser.*, **2857**, 012032 (2024). <https://doi.org/10.1088/1742-6596/2857/1/012032>.
9. H. Eyidoğan, *Tectonophysics*, **148**, 83 (1988). [https://doi.org/10.1016/0040-1951\(88\)90162-X](https://doi.org/10.1016/0040-1951(88)90162-X).

10. F. J. Glago, Nat. Hazards-Impacts, **29**, 37 (2021). <http://dx.doi.org/10.5772/intechopen.77525>.
11. Zhu, Lingjie, Xing, Xuemin Zhu, Yikai Peng, Wei Yuan, Zhihui, and Xia, Qing, IEEE J. Sel. Top. Appl. Earth Obs. Remote Sens., **14**, 7682 (2021). <https://doi.org/10.1109/JSTARS.2021.3100086>.
12. Abd Jasim and M. A. Hassan, Iraqi Geol. J., **93**, 113 (2020). <https://doi.org/10.46717/igi.53.1D.7Rw-2020-05.06>.
13. A. Jasim, Ph.D. Thesis, Univ. Baghdad, 2021.
14. A. H. Sayyid, A. H. Shaban, and N. A. Abd, AIP Conf. Proc., **3018**, 012025 (2023). <https://doi.org/10.1063/5.0171975>.
15. A. H. Sayyid, A. H. Shaban, and N. A. Abd, Iraqi J. Sci., **65**, 5339 (2024). <https://doi.org/10.24996/ijs.2024.65.9.43>.
16. C-P Chang, J-Y Yen, A. Hooper, F-M Chou, Y-A Chen, C-Sh Hou, W-C Hung, and M-Sh Lin, Terr. Atmos. Oceanic Sci., **21**(3), 447 (2010). [https://10.3319/TAO.2009.11.20.01\(TH\)](https://10.3319/TAO.2009.11.20.01(TH)).
17. M. Shirzaei, T.R. Walter, H.R. Nankali, and E.P. Holohan, Geology, **39**, 251 (2011). <https://10.1130/G31779.1>.
18. G. Wöppelmann, G. L. Cozannet, M. De Michele, D. Raucoules, A. Cazenave, M. Garcin, S. Hanson, M. Marcos, and A. Santamaría-Gómez, Geophys. Res. Lett., **40**, 2953 (2013). <https://10.1002/grl.50568>.
19. P. Milillo, M. C. Porcu, P. Lundgren, F. Soccodato, J. Salzer, E. Fielding, R. Bürgmann, G. Milillo, D. Perissin, and F. Biondi, International Geoscience and Remote Sensing Symposium IGARSS, 6279 (2017). <https://10.1109/IGARSS.2017.8128442>.
20. J. Shi, B. Xu, Q. Chen, M. Hu, and Y. Zeng, Int. J. Appl. Earth Obs. Geoinf., **107**, 102679 (2022). <https://doi.org/10.1016/j.jag.2022.102679>.
21. L. Xu, Y. Yang, X. Ju, and J. Yang, Front. Earth Sci., **10**, 983155 (2023). <https://doi.org/10.3389/feart.2022.983155>.
22. N. N. Almaalei and S. N. A. M. Razali, Int. J. Adv. Comput. Sci. Appl., **10**, 11 (2019).
23. M. Jiyad, Int. J. Contemp. Iraqi Stud., **4**, 155 (2010). https://doi.org/10.1386/ijcis.4.1&2.155_1.
24. A. Kubursi, Arab Stud. Q., 283 (1988).
25. S. M. Awadh and H. Al-Mimar, Geogr. Iraq, 333 (2024). https://doi.org/10.1386/ijcis.12.3.319_1.
26. A. M. Handhal, H. A. Chafeet, and H. A. Subber, J. Basrah Res. Sci., **42** و A (2016). <http://www.basra-science-journal.org>.
27. R. J. Zedalis, Eur. J. Int. Law, **18**, 499 (2007). <https://doi.org/10.1093/ejil/chm026>.
28. K. Al-Mehaidi, Revenue Watch Inst., 21-22 (2006).
29. DIVA-GIS, https://diva-gis.org.
30. L. Zhang, X. Ding, and Z. Lu, Int. J. Image Data Fusion, **6**, 289 (2015). <https://doi.org/10.1080/19479832.2015.1068874>.
31. M. Mourjane, H. Tabyaoui, and F. El Hammichi, Dev. Environ. Sci., **16**, 415 (2024). <https://doi.org/10.1016/B978-0-443-23665-5.00017-X>.
32. OPEC, Annual Report, Vienna, Austria, 2017-2022. [Online]. Available: https://www.opec.org/opec_web/en/

حسابات تشوه سطح الأرض بسبب استخراج النفط في حقل الرميلة النفطي في العراق باستخدام *DInSAR*

علي اياد حسين¹ عدي حاتم شعبان¹ ونجاح عبد الحسن عبد²

¹ قسم التحسس النائي ونظم المعلومات الجغرافية، كلية العلوم، جامعة بغداد، بغداد، العراق

² قسم علوم الارض، كلية العلوم، جامعة بغداد، بغداد، العراق

الخلاصة

إن استخراج النفط صناعة حيوية بالنسبة للعراق، حيث تساهم بشكل كبير في اقتصاد البلاد، وخاصة في محافظة البصرة. ومع ذلك، فإن أنشطة الاستخراج المكثفة يمكن أن تؤدي إلى تشوه الأرض، والذي يتجلى في كل من الهبوط والارتفاع، مما قد يؤثر على البنية التحتية والبيئة. تبحث هذه الدراسة في تشوه الأرض الناجم عن استخراج النفط في حقل الرميلة النفطي، أحد مناطق إنتاج النفط الرئيسية في العراق، والذي يقع في جنوب العراق. لتحليل هذه التشوهات، استخدمت الدراسة تقنيات الرادار ذي الفتحة الاصطناعية التفاضلية التداخلية (DInSAR) باستخدام بيانات Sentinel-1 SAR من وكالة الفضاء الأوروبية. يسمح DInSAR بقياس دقيق لتشوه السطح من خلال حساب فروق الإزاحة بين أزواج صور الرادار ذي الفتحة الاصطناعية بمرور الوقت، مما يجعله أداة فعالة لمراقبة الحركات الأرضية الدقيقة. تم اختيار حقل الرميلة النفطي، الذي يتكون من أقسام شمالية وجنوبية، بسبب إنتاجه النفطي المرتفع وأهميته للاقتصاد العراقي. تكشف النتائج عن تشوه كبير في حقل الرميلة النفطي، مع معدل هبوط أقصى يبلغ حوالي -1.67 مترًا على مدى ست سنوات. أظهر حقل الرميلة الجنوبي تشوهات أكثر جوهريّة، وهو ما يرتبط بمعدلات استخراج أعلى، في حين أظهر الحقل الشمالي تشوهات طفيفة نسبيًا بسبب مستويات الاستخراج المنخفضة. ويسلط هذا التمييز الضوء على تأثير كثافة الاستخراج على استقرار الأرض داخل الحقل.

الكلمات المفتاحية: التشوه، الرميلة، الاستشعار عن بعد، InSAR، حقل النفط.